

# DEVELOPMENT OF $d$ - $q$ WPT-BASED DIGITAL PROTECTION FOR SYMMETRICAL FAULTS OCCURRING DURING POWER SWINGS

DEVI.R<sup>1</sup>

N.SHANMUGA VADIVOO<sup>2</sup>

<sup>1</sup>Department of Electrical and Electronics Engineering, Sri Krishna College of Technology,  
Coimbatore-641042, India, shaaa.nthidevi@gmail.com

<sup>2</sup>Department of Electrical and Electronics Engineering, Thiagarajar College of Engineering,  
Madurai-625015, India  
nsveee@tce.edu

**Abstract**— This paper presents the performance evaluation of a new digital protection for symmetrical faults occurred during the occurrence of power swing. The proposed digital protection is based on extracting the first level low frequency and high frequency sub-band contents present in the  $d$ - $q$  -axis three phase instantaneous current components. This characterization helps to provide enough information to efficiently detect and discriminate power swing and symmetrical faults during power swing in two machine system. The utilized Wavelet Packet Transform (WPT) is realized by a half-band digital low and high pass filter, whose coefficients are determined by the Daubechies db4 wavelet basis functions. The WPT coefficients contain information that offer accurate, fast, and reliable detection in discriminating power swing and symmetrical fault. This detection method is immune to the power swing slip frequency, fault inception time and fault location. To test the proposed method, several power swings and faults are numerically simulated in MATLAB/SIMULINK.

**Key words:** Digital protective relays,  $d$ - $q$ -axis components, power swing, symmetrical fault, wavelet packet transform and transient disturbances.

## NOMENCLATURE

$x_d[n]$	Discrete signal
WT	Wavelet Transform
WPT	Wavelet Packet Transform
$d$ - $q$	Direct-and- quadrature -axis rotating reference frame
$j$	Level of decomposition in WT and WPT
$A_{j,k}[n]$	Low frequency content present in $x_d[n]$
$D_{j,k}[n]$	High frequency content present in $x_d[n]$

$A1dq[n]$	First level low frequency subband of $dq$ – WPT
$I_a[n], I_b[n], I_c[n]$	Current components of 3 $\phi$ signal
$D1dq[n]$	First level high frequency subband of $dq$ – WPT
$\Psi$	Non- zero value of $D1dq[n]$
$Dad3[n]$	Third- level subband frequencies (high- low- high) of phase A current
$Dda3[n]$	Third- level subband frequencies (high- high-low) of phase A current
DFT	Discrete Fourier Transform
FFT	Fast Fourier Transform
$I_d[n]$	Direct axis current
$I_q[n]$	Quadrature axis current
$\Omega_1, \Omega_2, \Omega_3$	Continuous frequency components in rad/sec
$g[n]$	Low pass filter coefficients
$h[n]$	High pass filter coefficients
$B_L$	Low frequency half band
$B_H$	High frequency half band
$\omega_1, \omega_2, \omega_3, \omega_4, \omega_s$	Discrete frequencies
$\lambda I$	Threshold
$\lambda$	Non zero value of $A1dq[n]$
$M$	Length of filter
db <sub>4</sub>	Daubechies 4 wavelet
$f_1, f_2, f_s$	Continuous frequencies in Hz
$V_m$	Maximum value of voltage
$\theta_A$	Phase angle of input voltage
$R$	Resistance
$L$	Inductance
$T$	Transformation matrix

P	Park transformation
$\alpha_a, \alpha_b, \alpha_c$	Time functions of $3\phi$ quantities
$\alpha_d, \alpha_q, \alpha_0$	Time functions of $d - q0$ components
$T_s$	Sampling time

## 1. Introduction

Distance relays used for transmission line protection operate on the basis of measured apparent impedance. Power swing cause change in electrical load impedance under steady state condition. During power swing, the apparent impedance measured by a distance relay may move in to the tripping zone of the distance relay characteristics, causing unnecessary trip [1]. Power swing creates oscillations in active and reactive powers following severe disturbances such as line faults, loss of generation and switching heavy loads.

Asymmetrical faults are unbalanced and it produces negative and zero sequence components, makes it possible to detect fault during the power swing. During symmetrical fault and power swing, these components are not present. Symmetrical fault is the most severe fault involving largest current and it occurs rarely compared to unsymmetrical fault. It is difficult for distance relay to distinguish a power swing from a symmetrical fault. To detect symmetrical faults during power swing, several methods have been proposed [2]. It is not possible to detect symmetrical fault occurs during a power swing based on negative and zero sequence components because both power swing and symmetrical fault are both balanced phenomena in [3]. The basic theory of relay to distinguish the power swing from a fault is the speed of impedance moving during the power swing is slower than during the fault condition.

In [4], Fast Fourier Transform (FFT) is used to detect symmetrical fault using frequency components of instantaneous three phase active power, the minimum time required is half cycle and 1 kHz sampling frequency is required. Su *et al.* [5] used swing center voltage (SCV) to detect symmetrical faults occurred during power swing. Lin *et al.* [6] presented a method for detecting symmetrical faults by measuring three-phase active and reactive powers. Lotfifard *et al.* [7] presented a method based on the dc component of three-phase currents, extracted by the Prony method.

Wavelet-based signal-processing techniques are effective tools for power system transient analysis [8-10].

Several fault detection methods based on the wavelet transform (WT) are proposed in [2, 3, 11]. In [2], Brahma introduced the use of WT to detect the symmetrical fault, but the sampling rate of 40.96 kHz is needed to satisfy all of the studied cases. In [3], traveling wave based protection along with WT is used. High sampling rate of 10 kHz and 5<sup>th</sup> level decomposition is used to detect symmetrical fault with fault detection time of 3 ms. In [11], 20 kHz sampling rate and 8<sup>th</sup> level wavelet decomposition is used to detect fault and power swing with the response time for fault detection is 1.5 cycles which is slow.

Performances of WPT-based digital and micro-processor based protective relays have demonstrated significant capabilities for identifying and responding to faults in [12,13].

The  $d-q$  WPT-based digital relays have been tested for power transformers, motor drives and micro-grids [14-17]. This  $d-q$  WPT-based digital protection method has shown simplified realization without compromising the accuracy and speed of response. In this paper, the WPT in the  $d-q$ -axis reference frame has been used to detect symmetrical fault during power swing. Power swing is low frequency oscillation which can be detected by using first level approximation of  $d-q$  WPT whereas symmetrical fault is high frequency oscillation which can be detected by using first level details  $d-q$  WPT.

## 2. The $d-q$ WPT-Based Disturbance Detection and Classification Method

### 2A. Wavelet packet transform

The WPT is one of the most effective and accurate methods for processing signals associated with transient disturbances. It provides extended signal decomposition and it is used to extract frequency contents of the processed signal over narrow frequency sub-bands. Decomposition of the discrete signal  $x_d[n]$  using WPT is shown in Fig.1.

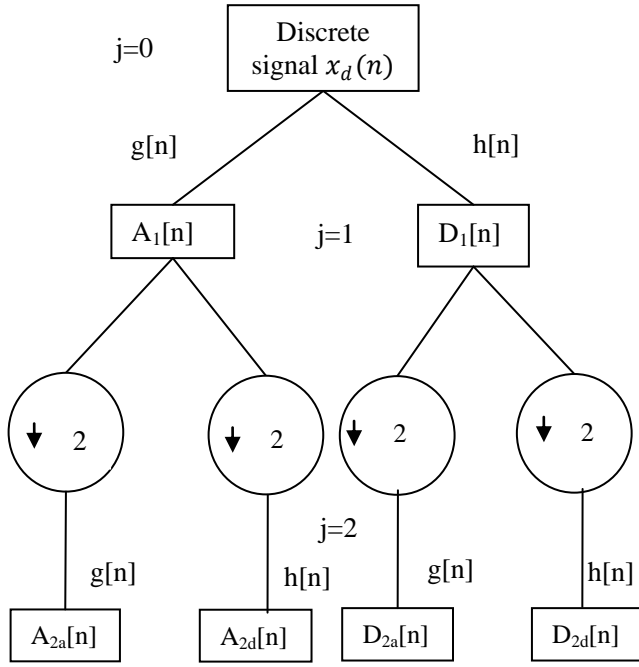


Fig.1. Decomposition of discrete signal using wavelet packet transform (WPT)

This type of signal processing can be expressed for a discrete signal as

$$x_d[n] = \sum_{j \in \mathbb{Z}} \sum_{k \in \mathbb{Z}} A_{j,k}[n] + \sum_{j \in \mathbb{Z}} \sum_{k \in \mathbb{Z}} D_{j,k}[n] \quad (1)$$

where  $A_{j,k}[n]$  and  $D_{j,k}[n]$  are given by

$$A_{j,k}[n] = \sum_{j \in \mathbb{Z}} (g[k] A_{(j-1)}[2n-k] + h[k] A_{(j-1)}[2n-k]) \quad (2)$$

$$D_{j,k}[n] = \sum_{j \in \mathbb{Z}} (g[k] D_{(j-1)}[2n-k] + h[k] D_{(j-1)}[2n-k]) \quad (3)$$

The approximations  $A_{j,k}[n]$  represents the low frequency content present in  $x_d[n]$  at scale  $j$ , and the details represents the high frequency content present in  $x_d[n]$  at scale  $j$ . The equations (1)-(3) are taken from [13,16,17]. The set  $g[k]$  and  $h[k]$  are the low pass filter (LPF) and high pass filter (HPF) coefficients respectively.

## 2B. d-q WPT-based transient detection and classification

In [12,14,17], frequency components associated with non-fault transient (magnetizing inrush, load changes, stable power swing, motor starting, etc.) will be relocated in Low frequency half band  $B_L$ . Frequency components associated with fault transient, will be relocated in between  $B_L$  and high frequency half

band  $B_H$ . The power swing and fault transient disturbances generated will have non-zero WPT coefficients for the low and high frequency sub-band extracted from  $d-q$  axis components respectively. In [17], the advantages of this  $0dq$ -WPT technique are as follows.

- High sampling frequency is not required by using the  $d-q$  axis components.
- By changing the three phase sinusoidal signals to dc signals, the implementation complexity, the computational burden and memory requirements are reduced.
- It is not sensitive to the non-periodicity of the signal

The  $0dq$  components are given by

$$\begin{bmatrix} \alpha_d(t) \\ \alpha_q(t) \\ \alpha_0(t) \end{bmatrix} = T \begin{bmatrix} \alpha_a(t) \\ \alpha_b(t) \\ \alpha_c(t) \end{bmatrix} \quad (4)$$

where  $\alpha_a(t)$ ,  $\alpha_b(t)$ , and  $\alpha_c(t)$  are  $3\phi$  quantities (currents or voltages) and park transformation matrix  $T$  is given by

$$T = \sqrt{\frac{2}{3}} \begin{bmatrix} \cos \delta & \cos(\delta - \frac{2\pi}{3}) & \cos(\delta + \frac{2\pi}{3}) \\ \sin \delta & \sin(\delta - \frac{2\pi}{3}) & \sin(\delta + \frac{2\pi}{3}) \\ \frac{1}{\sqrt{2}} & \frac{1}{\sqrt{2}} & \frac{1}{\sqrt{2}} \end{bmatrix} \quad (5)$$

where angle  $\delta = 2\pi f_s t = \Omega_s t$  with  $f_s$  being the fundamental frequency in  $\alpha_a(t)$ ,  $\alpha_b(t)$ , and  $\alpha_c(t)$ .

The equations (4) and (5) are taken from [17]. The relocation of frequencies can be illustrated if one considers two frequencies  $f_1$  and  $f_2$ , such that  $f_1 < f_s$  and  $f_2 > f_s$ . In [12], these frequencies will be relocated by the  $abc$ -to- $dq0$  transformation as shown in Fig.2.

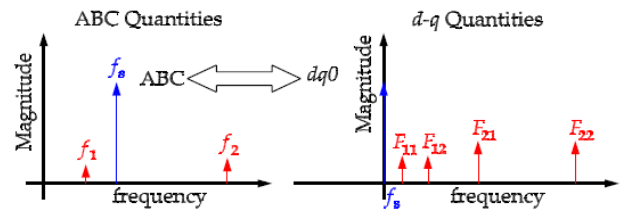


Fig.2. Mapping and relocating frequencies using  $abc$ -to- $dq0$  transformation

Relocating and converting continuous frequency components present in 3 phase quantities to discrete frequencies of the  $d-q$  axis components is shown in Fig.3. Mapped and relocated discrete frequencies  $\omega_1$  and  $\omega_2$  are related to  $f_1$ , whereas  $\omega_3$  and  $\omega_4$  are related to  $f_2$ .

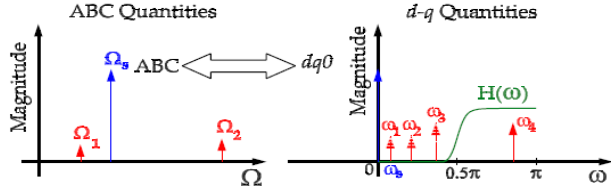


Fig.3. Relocating continuous frequency components to discrete frequencies of the  $d-q$  axis components

The Transformation P in [13] relocates all frequency components present in  $\alpha_a(t)$ ,  $\alpha_b(t)$  and  $\alpha_c(t)$ , and so that

$$f_s \xleftrightarrow{P} [0 = |f_s - f_s|] \quad (6)$$

$$f_1 \xleftrightarrow{P} \begin{cases} F_{11} = |f_1 - f_s| \\ F_{12} = |f_1 + f_s| \end{cases} \quad (7)$$

$$f_2 \xleftrightarrow{P} \begin{cases} F_{21} = |f_2 - f_s| \\ F_{22} = |f_2 + f_s| \end{cases} \quad (8)$$

Low frequency half-band  $B_L : 0 \leq \omega < \frac{\pi}{2}$

High frequency half-band  $B_H : \frac{\pi}{2} \leq \omega < \pi$

$$A_{dq}[n] = \begin{cases} 0, & \text{Normal} \\ \psi(\text{sinusoidal}), & \text{power swing} \end{cases} \quad (9)$$

$$D_{dq}[n] = \begin{cases} \psi \leq \lambda 1, & \text{Non - Fault} \\ \psi > \lambda 1, & \text{Fault} \end{cases} \quad (10)$$

where  $\lambda 1$  is threshold

$A_{dq}[n]$  using circular convolution operation is given by

$$A_{dq}[n] = \sum_{k=0}^{M-1} g[k]X_{dq}[n-k] \quad (11)$$

$D_{dq}[n]$  using circular convolution operation is given by

$$D_{dq}[n] = \sum_{k=0}^{M-1} h[k]X_{dq}[n-k] \quad (12)$$

where M is the length of  $h[k]$  and  $g[k]$ .  $M=8$

$X_{dq}[n]$  is given as:

$$X_{dq}[n] = (I_d[n])^2 + (I_q[n])^2 \quad (13)$$

where  $I_d[n]$  and  $I_q[n]$  are the  $d-q$ -axis components of the  $3\phi$  components. These components are calculated using the following equations.

$$I_d[n] = \sqrt{\frac{2}{3}}(I_a[n] \cos(\delta) + I_b[n] \cos(\delta - \frac{2\pi}{3}) + I_c[n] \cos(\delta + \frac{2\pi}{3})) \quad (14)$$

$$I_q[n] = \sqrt{\frac{2}{3}}(I_a[n] \sin(\delta) + I_b[n] \sin(\delta - \frac{2\pi}{3}) + I_c[n] \sin(\delta + \frac{\pi}{3})) \quad (15)$$

The Daubechies  $db4$  is employed as wavelet basis functions as in [12]. The eight coefficients of  $db4$  of the LPF and the HPF are as follows:

$$g[k] = [-0.0106 \ 0.0329 \ 0.0308 \ -0.1870 \ -0.0280 \ 0.6309 \ 0.7148 \ 0.2308] \quad (16)$$

$$h[k] = [-0.2304 \ 0.715 \ -0.631 \ -0.028 \ 0.187 \ 0.031 \ -0.0329 \ 0.0106] \quad (17)$$

### 3. Proposed Symmetrical Fault Detection Method

A flowchart of the proposed method in a logical pattern is shown in Fig.4.  $0dq$  transformation is performed on instantaneous three phase currents and WPT is performed on  $d-q$  components.

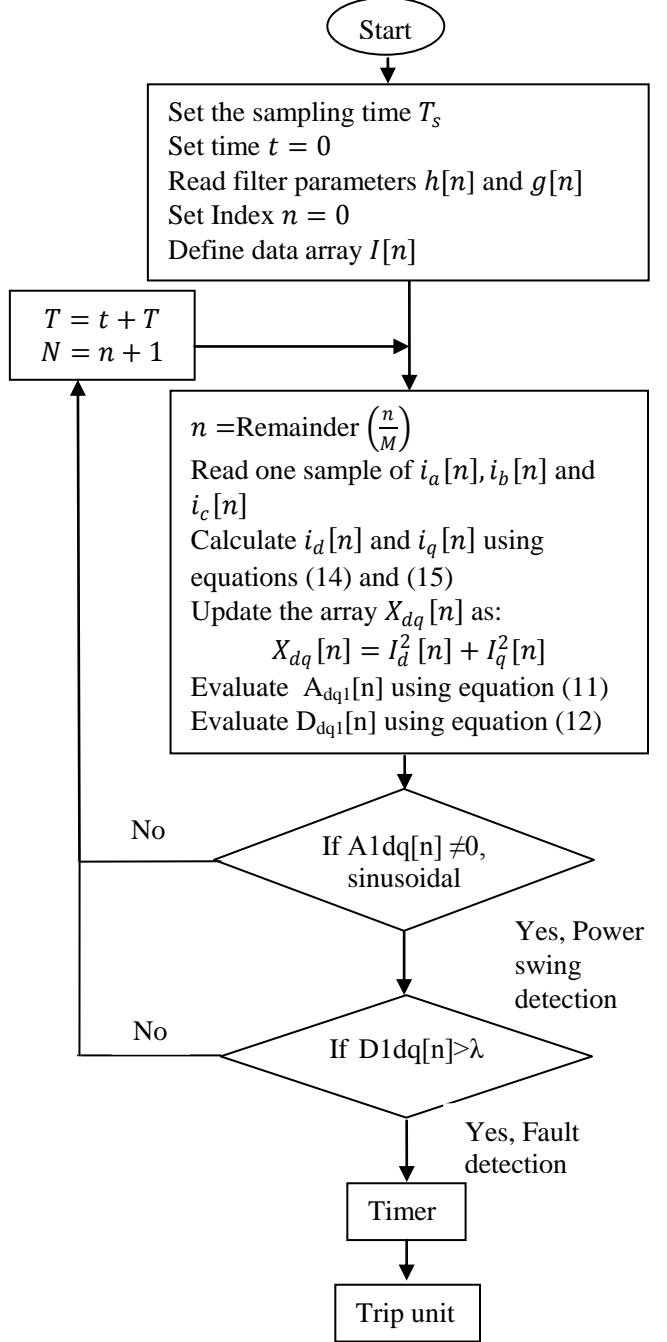


Fig.4. Flowchart for the proposed method

If the  $D_{1dq}[n]$  is greater than threshold, then fault is detected. If  $A_{1dq}[n]$  is not equal to zero, power swing is detected. This method is insensitive for fault distance, and power swing slip frequency.

### 3A. Two machine system

In a double frequency system, during power swing, the three-phase current oscillates at the slip frequency. After the fault inception, it oscillates at the nominal frequency (50 or 60Hz). To demonstrate the proposed symmetrical fault detection method, a series of tests by using MATLAB/SIMULINK to a two machine 400-kV transmission system [4] shown in Fig.5. was conducted. The length of the transmission line is 150 km. Symmetrical faults are applied on various distances on transmission line. The system details are given in the Appendix. Table 1 indicates the different cases fault simulation with different values of power swing taken from [4]. The sampling frequency chosen is 2 kHz. If sampling frequency is further increased, the speed of fault detection will be increased. The WPT is carried out every 0.5 ms. The fault can then be detected in quarter power cycle.

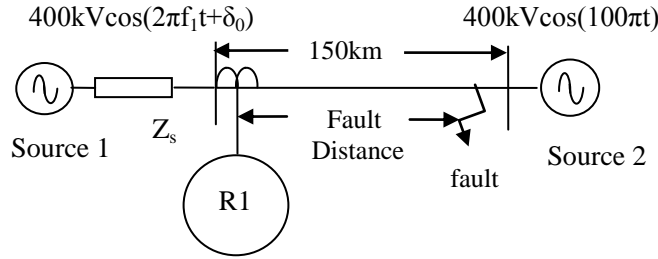


Fig.5. Simulated two machine system.

### 3B. Three phase currents after symmetrical fault inception

To extract the phase currents during symmetrical fault, lumped model for faulty system is used.

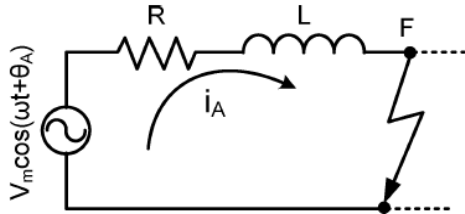


Fig.6. Lumped model for Phase A after symmetrical fault inception

Fig.6. shows the model for phase A when symmetrical fault occurs [4].  $V_m \cos(\omega t + \theta_A)$  is the input voltage for the lumped model.  $i_A$  is current flowing through the circuit.

The phase A current is governed by equation

$$Ri_A + L \frac{di_A}{dt} = V_m \cos(\omega t + \theta_A) \quad (18)$$

$$i_A(t) = K_{1A} e^{-\left(\frac{R}{L}\right)t} + \frac{V_m}{\sqrt{R^2 + L\omega^2}} \sin(\omega t + \beta_A) \quad (19)$$

where  $\beta_A$  can be found by

$$\beta_A = \tan^{-1} \left( \frac{R \cos \theta_A + \omega L \sin \theta_A}{\omega L \cos \theta_A - R \sin \theta_A} \right) \quad (20)$$

Where  $K_{1A}$  is a constant obtained from the initial condition by

$$K_{1A} = i_A(0) - \left( \frac{V_m}{R^2 + L\omega^2} \right) \sin \beta_A \quad (21)$$

Phase B and C currents can be written accordingly as

$$i_B(t) = K_{1B} e^{-\left(\frac{R}{L}\right)t} + \frac{V_m}{\sqrt{R^2 + L\omega^2}} \sin(\omega t + \beta_B) \quad (22)$$

$$i_C(t) = K_{1C} e^{-\left(\frac{R}{L}\right)t} + \frac{V_m}{\sqrt{R^2 + L\omega^2}} \sin(\omega t + \beta_C) \quad (23)$$

$$\beta_B = \beta_A - \frac{2\pi}{3} \quad (24)$$

$$\beta_C = \beta_A + \frac{2\pi}{3} \quad (25)$$

$$K_{1B} = i_B(0) - \left( \frac{V_m}{R^2 + L\omega^2} \right) \sin \beta_B \quad (26)$$

$$K_{1C} = i_C(0) - \left( \frac{V_m}{R^2 + L\omega^2} \right) \sin \beta_C \quad (27)$$

Table 1

Simulated cases of two machine system for evaluating the proposed method

Case	Power swing slip frequency (Hz)	Fault distance to relay R1(km)	Fault inception time (s)
1	1	5	1.50
2	1	75	1.75
3	1	145	2.00
4	2	5	0.75
5	2	75	0.87
6	2	145	1.00
7	3	5	0.83
8	3	75	0.91
9	3	145	1.00
10	4	5	0.62
11	4	75	0.68
12	4	145	0.75
13	5	5	0.50

#### 4. Simulation results of two machine system

The simulation results of the two machine system for the different cases in Table 1 are shown in the following figures.

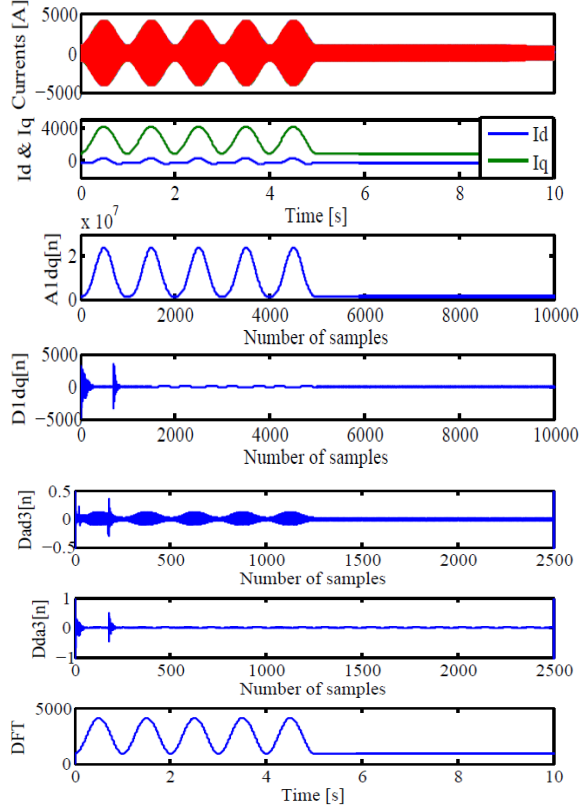


Fig.7. Three phase currents,  $d-q$  -axis components  $I_d$  and  $I_q$ , Low -frequency sub band  $A1dq[n]$ , high -frequency sub band  $D1dq[n]$ ,  $Dda3[n]$  and  $Dad3[n]$  of WPT, DFT of phase A current measured during power swing slip frequency of 1Hz

In Fig.7. the  $A1dq[n]$  is having non zero sinusoidal oscillations and it indicates the presence of power swing during time period 1-5s. For normal conditions,  $A1dq[n]$  is zero and it indicates there is no power swing during the time duration 5-10s. The results show that the first stage approximation  $A1dq[n]$  itself detects the power swing. The details  $D1dq[n]$  shows the impulse signal at the starting and end of the swing. Hence,  $A1dq[n]$  is used to detect power swing and  $D1dq[n]$  is used to detect the fault. Due to the impulse signal at the starting and end of the swing, a threshold is fixed to operate for fault condition.

In WPT method, the  $Dad3[n]$  indicates the sinusoidal signal during power swing, the  $Dda3$  does not

detect the power swing. Hence,  $Dad3[n]$  is used to detect power swing and  $Dda3[n]$  is used to detect fault condition. In DFT method, the DFT signal indicates the sinusoidal signal during power swing and for the remaining time duration, the DFT signal has constant magnitude.

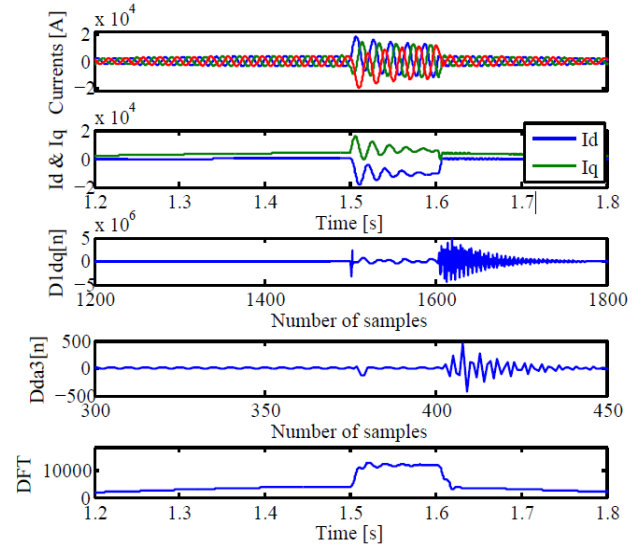


Fig.8. Three phase currents,  $d-q$  -axis components  $I_d$  and  $I_q$ , High-frequency sub-band  $D1dq[n]$ ,  $Dda3[n]$  of WPT and DFT of phase A current measured in case 1 in table 1

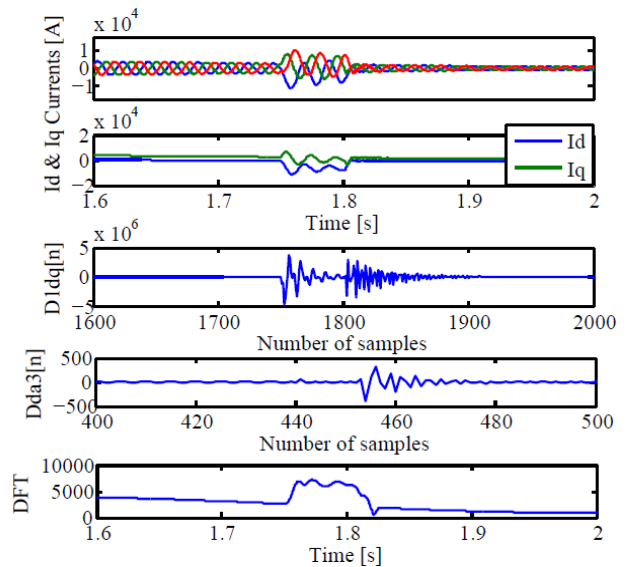


Fig.9. Three phase currents,  $d-q$  -axis components  $I_d$  and  $I_q$ , High-frequency sub-band  $D1dq[n]$ ,  $Dda3[n]$  of WPT and DFT of phase A current measured in case 2 in table 1

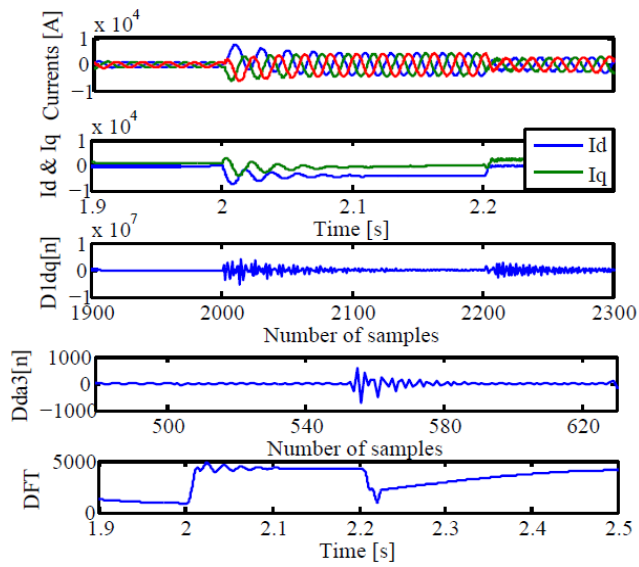


Fig.10. Three phase currents,  $d-q$  -axis components  $I_d$  and  $I_q$ , High-frequency sub-band  $D1dq[n]$ ,  $Dda3[n]$  of WPT and DFT of phase A current measured in case 3 in table 1

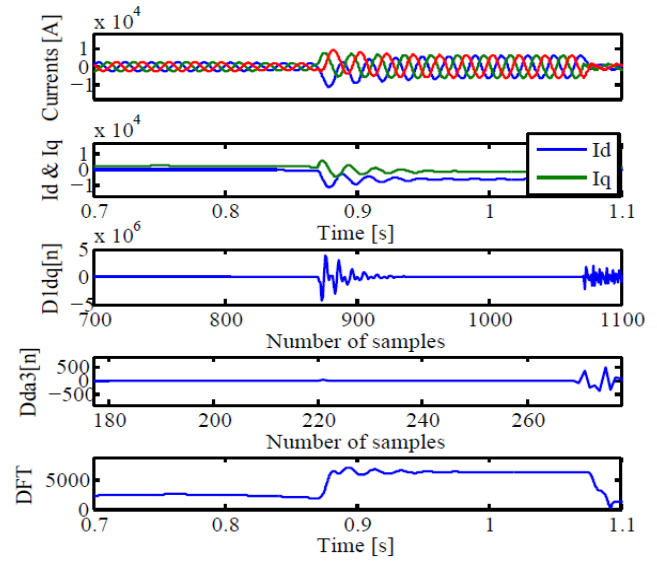


Fig.12. Three phase currents,  $d-q$  -axis components  $I_d$  and  $I_q$ , High-frequency sub-band  $D1dq[n]$ ,  $Dda3[n]$  of WPT and DFT of phase A current measured in case 5 in table 1

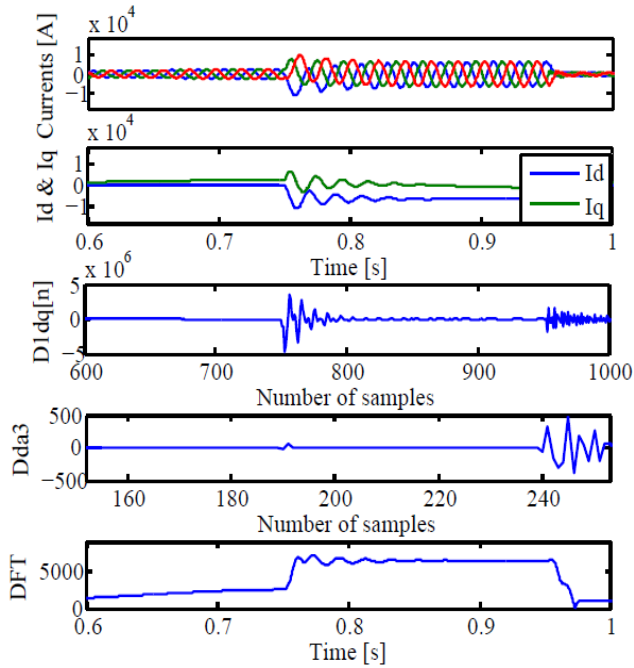


Fig.11. Three phase currents,  $d-q$  -axis components  $I_d$  and  $I_q$ , High-frequency sub-band  $D1dq[n]$ ,  $Dda3[n]$  of WPT and DFT of phase A current measured in case 4 in table 1

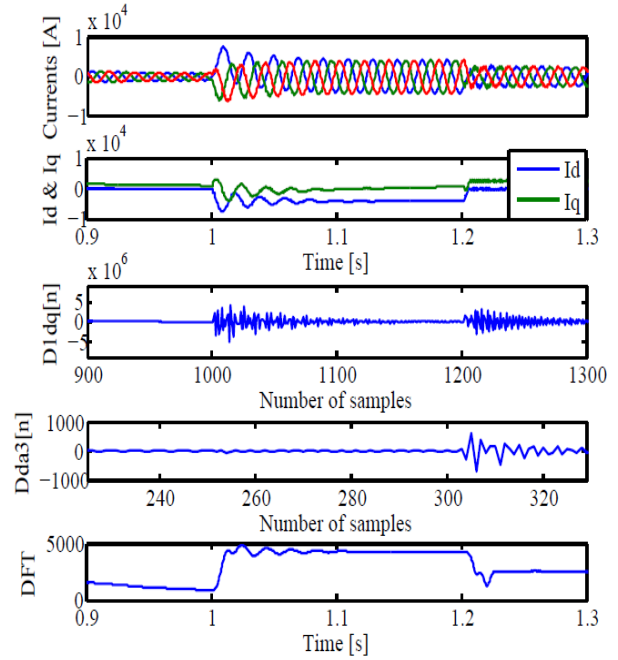


Fig.13. Three phase currents,  $d-q$  -axis components  $I_d$  and  $I_q$ , High-frequency sub-band  $D1dq[n]$ ,  $Dda3[n]$  of WPT and DFT of phase A current measured in case 6 in table 1

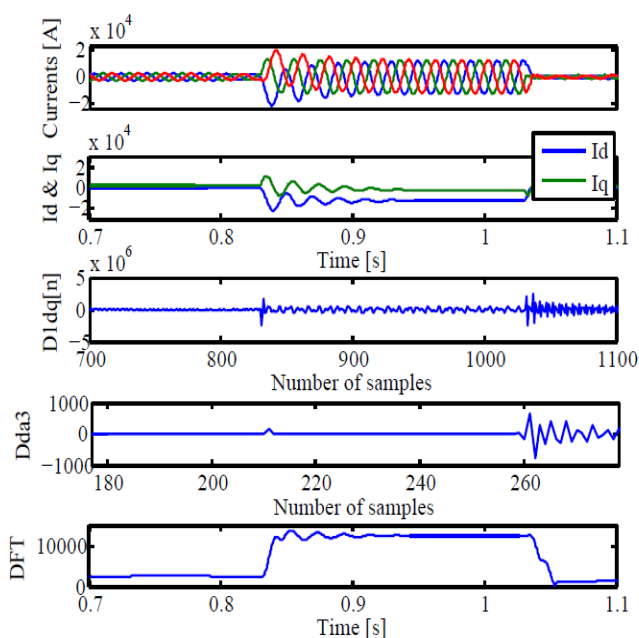


Fig.14. Three phase currents,  $d-q$  -axis components  $I_d$  and  $I_q$ , High-frequency sub-band  $D1dq[n]$ ,  $Dda3[n]$  of WPT and DFT of phase A current measured in case 7 in table 1

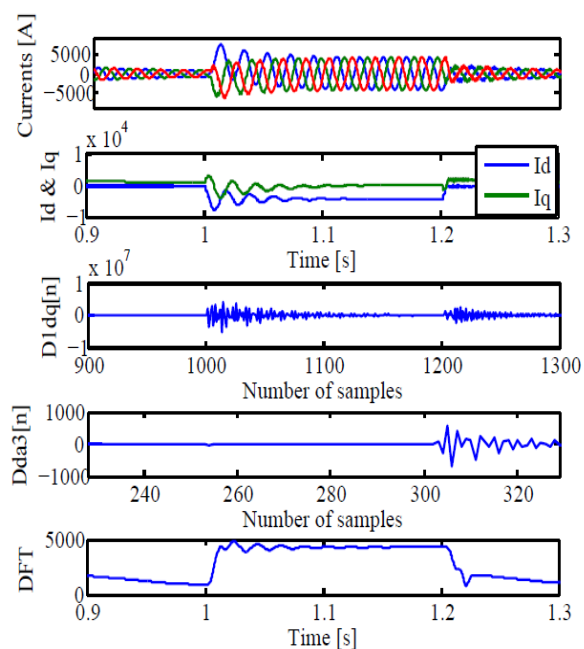


Fig.16. Three phase currents,  $d-q$  -axis components  $I_d$  and  $I_q$ , High-frequency sub-band  $D1dq[n]$ ,  $Dda3[n]$  of WPT and DFT of phase A current measured in case 9 in table 1

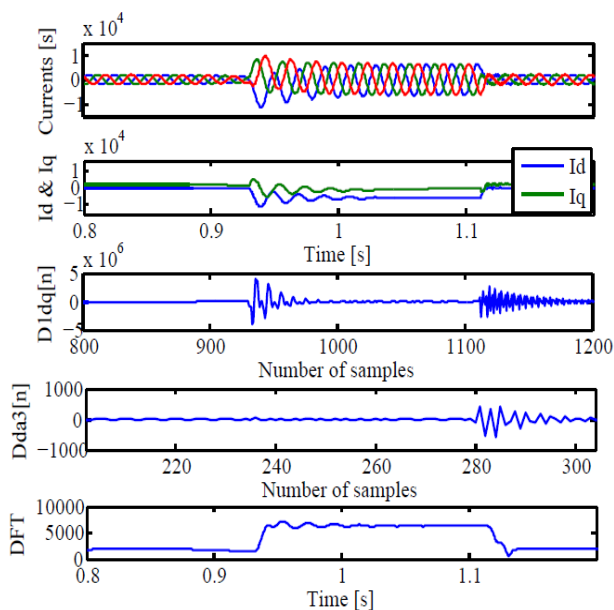


Fig.15. Three phase currents,  $d-q$  -axis components  $I_d$  and  $I_q$ , High-frequency sub-band  $D1dq[n]$ ,  $Dda3[n]$  of WPT and DFT of phase A current measured in case 8 in table 1

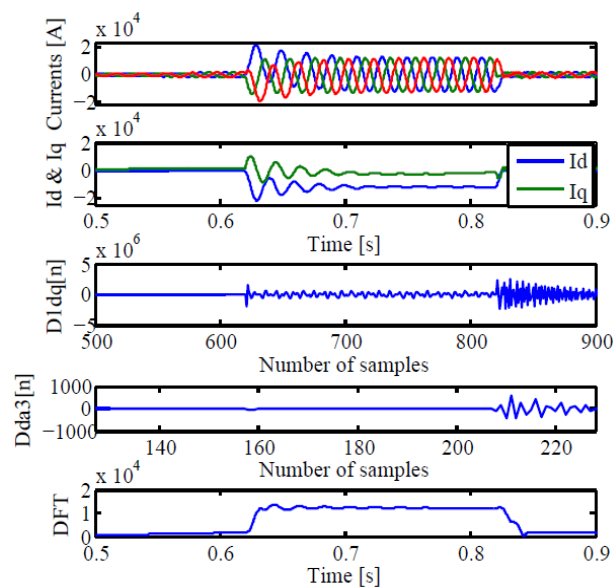


Fig.17. Three phase currents,  $d-q$  -axis components  $I_d$  and  $I_q$ , High-frequency sub-band  $D1dq[n]$ ,  $Dda3[n]$  of WPT and DFT of phase A current measured in case 10 in table 1

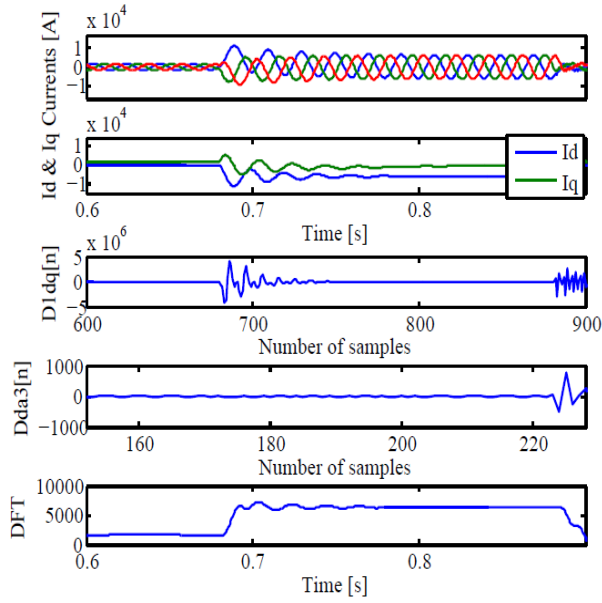


Fig.18. Three phase currents,  $d-q$  -axis components  $I_d$  and  $I_q$ , High-frequency sub-band  $D1dq[n]$ ,  $Dda3[n]$  of WPT and DFT of phase A current measured in case 11 in table 1

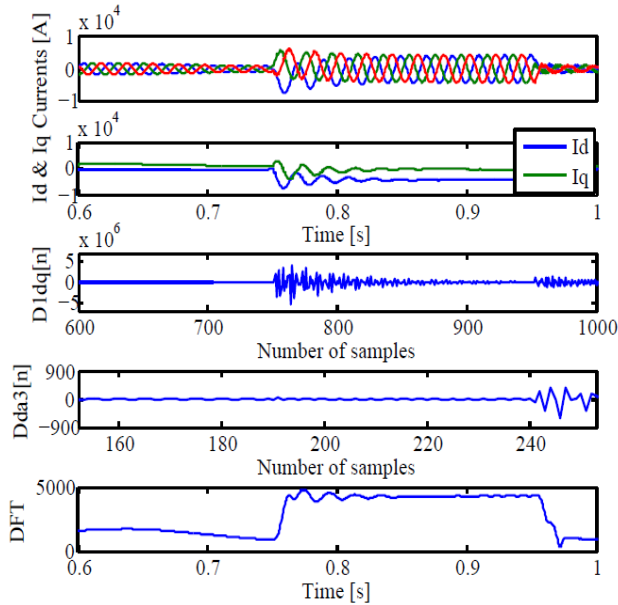


Fig.19. Three phase currents,  $d-q$  -axis components  $I_d$  and  $I_q$ , High-frequency sub-band  $D1dq[n]$ ,  $Dda3[n]$  of WPT and DFT of phase A current measured in case 12 in table 1

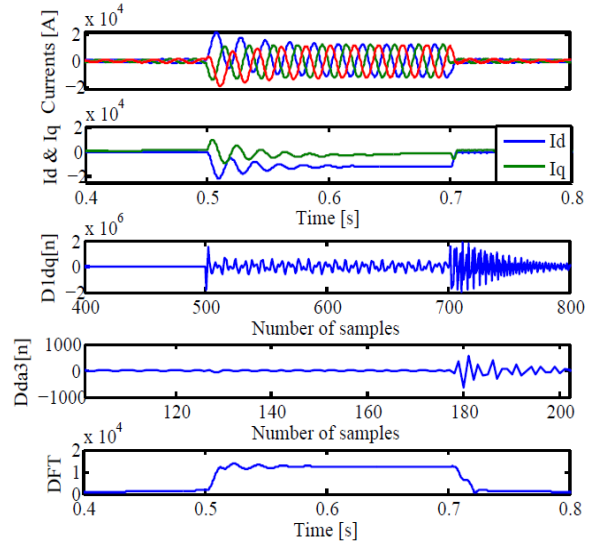


Fig.20. Three phase currents,  $d-q$  -axis components  $I_d$  and  $I_q$ , High-frequency sub-band  $D1dq[n]$ ,  $Dda3[n]$  of WPT and DFT of phase A current measured in case 13 in table 1

From Figs.8-20.  $D1dq[n]$  are non zero values for fault duration and it is zero for normal time durations. The first stage of  $D1dq[n]$  itself detects the symmetrical fault during power swing. In WPT method,  $Dda3$  signal is non-zero for symmetrical fault and zero for normal time durations and during power swing. In DFT method, the DFT coefficients are non zero for normal, power swing and fault conditions. But the values of coefficients during fault condition are high.

In Fig.7.  $D1dq[n]$  have considerable value during power swing conditions. Hence, threshold is necessary so that the relay will not operate for power swing. By comparing the  $D1dq[n]$  with a predetermined threshold  $\lambda$ , this method can detect a symmetric fault occurring during a power swing within quarter power cycle. The threshold value was determined by a systematic numerical study of a series of cases for this power system. In two machine system, for all (1-13) cases, the maximum threshold value is 6000. i.e  $\lambda_1 = 6000$  for two machine system

$|D1dq[n]| > \lambda_1$ , fault is detected

$|D1dq[n]| < \lambda_1$ , fault is not detected

Comparisons of results are shown in table 2 and table 3.

Table 2

Comparison of results for various transforms for two machine system

Transforms	Normal	Power swing	Symmetrical fault during power swing
dq WPT	A1dq[n] is zero D1dq[n] is zero	A1dq[n] is non-zero sinusoidal oscillation, D1dq [n] is less than threshold	D1dq[n] is non-zero and greater than threshold
WPT	Dda3 is zero	Dad3 is non-zero sinusoidal oscillation, Dda3 is zero	Dda3 is non-zero
DFT coefficients	non-zero and constant value	sinusoidal oscillation	non-zero and it is greater that of normal

Table 3

Comparison of the  $d-q$  WPT, WPT and DFT Methods

Criterion	$d-q$ WPT	WPT	DFT
Sensitivity to Sampling Frequency	None	Sensitive	Sensitive
Inputs	$I_d$ and $I_q$	$i_a, i_b, i_c$	$i_a, i_b, i_c$
Analog implementation	1 HPF	3 LPFs and HPFs	3 LPFs
Inception angle	Insensitive	Insensitive	Sensitive
Level of Fault current	Insensitive	Insensitive	Sensitive
Memory requirement	Less	More	More

## 5. Conclusion

A novel scheme for detecting symmetrical faults occurring during power swings was presented based on the value of details of  $d-q$  -WPT coefficients of the three-phase currents after the fault inception within quarter power cycle. The presented digital protection has been structured to extract the high-frequency sub-band present in the  $d-q$ -axis components of the  $3\Phi$  currents. The proposed method has several advantages that are superior to the existing methods. The new method is very fast. While using a sampling frequency of only 2 kHz, it can detect the fault within quarter power cycle. Employment of a single-stage WPT, which has simplified the implementation and removed any constraints on the sampling frequency of measured currents. The  $d-q$  WPT-based digital protection has been simulated for performance evaluation on two machine system through a systematic numerical study of more than 10 disturbance conditions. In all tests, power swing frequency, fault locations have not affected responses of the  $d-q$  WPT-based digital protection. Finally, the  $d-q$  WPT-based digital protection has shown performance superiority over other digital protection methods in terms of response speed, simplicity, memory requirements. The distinct features and performance capabilities of the  $d-q$  WPT-based digital protection support its applications for discriminating power swing and symmetrical fault in two machine system.

## APPENDIX

The parameters of the two machine system used for simulation (Fig. 5) are given.

Source impedance

$$Z_{1S} = 2.21 + j25.04\Omega$$

$$Z_{0S} = 4.90 + j31.51\Omega$$

Transmission line: Distributed model with parameters

$$Z_{1L} = 0.03 + j0.34 \frac{\Omega}{km}$$

$$Z_{0L} = 0.28 + j1.04 \frac{\Omega}{km}$$

$$C_{1L} = 12.74 \frac{\mu F}{km}, C_{0L} = 7.75 \frac{\mu F}{km}$$

## References

1. Lotfifard S., Faiz J., Kezunovic M.: *Detection of symmetrical faults by distance relays during power swings*. In: IEEE Transactions on Power Delivery, Vol. 25, No. 1, 2010, p. 81–87.
2. Brahma, S. M.: *Distance relay with out-of-step blocking function using wavelet transform*. In: IEEE

- Transactions Power Delivery, Vol. 22, No. 3, 2007, p. 1360–1366.
3. Pang C., Kezunovic M.: *Fast distance relay scheme for detecting symmetrical fault during power swing*. In: IEEE Transactions on Power Delivery, Vol. 25, No. 4, 2010, p. 2205–2212.
  4. Mahamedi B., Zho J.: *A novel approach to detect symmetrical faults occurring during power swings by using frequency components of instantaneous three-phase active power*. In: IEEE Transactions on Power Delivery, Vol. 27, No. 3, 2012, p. 1368–1376.
  5. Su B., Dong X. Z., Bo Z. Q., Sun Y. Z., Caunce B. R. J., Tholomier D., Apostolov A.: *Fast detector of symmetrical fault during power swing for distance relay*. In: Proceedings of IEEE Power Engineering Society General Meeting, 2005, p. 1836–1841.
  6. Lin X., Gao Y., Liu P.: *A novel scheme to identify symmetrical faults occurring during power swings*. In: IEEE Transactions on Power Delivery, Vol. 23, No. 1, 2008, p. 73–78.
  7. Lotfifard S., Faiz J., Kezunovic M.: *Detection of symmetrical faults by distance relays during power swings*. In: IEEE Transactions on Power Delivery, Vol. 25, No. 1, 2010, p. 81–87.
  8. Santoso S., Powers E. J., Grady W. M., Hofmann P.: *Power quality assessment via wavelet transform analysis*. In: IEEE Transactions on Power Delivery, Vol. 11, No. 2, 1996, p. 924–930.
  9. Robertson D. C., Camps O. I., Mayer J. S., Gish W. B.: *Wavelets and electromagnetic power system transient*. In: IEEE Transactions on Power Delivery, Vol. 11, No. 2, 1996, p. 1050–1058.
  10. Michalik M., Rebizant W., Lukowicz M., Lee S. J., Kang S. H.: *High-impedance fault detection in distribution networks with use of wavelet-based algorithm*. In: IEEE Transactions on Power Delivery, Vol. 21, No. 4, 2006, p. 1793–1802.
  11. Dubey R., Samantaray S. R.: *Wavelet singular entropy-based symmetrical fault-detection and out-of-step protection during power swing*. In: IET Generation Transmission Distribution, Vol. 7, No. 10, 2013, p. 1123 – 1134.
  12. Saleh S. A., Aktaibi A., Ahshan R., Rahman M. A.: *The development of a d-q axis WPT-based digital protection for power transformers*. In: IEEE Transactions on Power Delivery, Vol. 27, No. 4, 2012, p. 2255-2269.
  13. Saleh S. A., Radwan T. S., Rahman M. A.: *Real-time testing of WPT-based protection of three-phase VS PWM inverter-fed motors*. In: IEEE Transactions on Power Delivery, Vol. 22, No. 4, 2007, p. 2108–2115.
  14. Saleh S. A., Ahshan R., Rahman M. A.: *Performance Evaluation of an Embedded d-q WPT-based digital protection for IPMSM drives*. In: IEEE Transactions on Industry Applications, Vol. 50, No. 3, 2014, p. 2277-2291,
  15. Saleh S. A., Rahman M. A.: *Real-time testing of WPT-based protection algorithm for three-phase power transformers*. In: IEEE Transactions on Industry Applications, Vol. 41, No. 4, 2005, p. 1125–1132.
  16. Saleh S. A., Rahman M. A.: *Modeling and protection of a three phase power transformer using wavelet packet transform*. In: IEEE Transactions on Power Delivery, Vol. 20, No. 2, 2005, p. 1273–1282.
  17. Adel Aktaibi M., Azizur Rahman., Azziddin Razali M., *An experimental implementation of the dq-Axis wavelet packet transform hybrid technique for three-phase power transformer protection*. In: IEEE Transactions on Power Delivery, Vol. 50, No. 4, 2014, p. 2919-2927.